**Research Article** **Open Access**

Achchhe Lal* and Niranjan L. Shegokar

# Thermoelectrically induced nonlinear free vibration analysis of piezo laminated composite conical shell panel with random fiber orientation

DOI 10.1515/cls-2017-0016
Received Jan 01, 2017; accepted Jun 09, 2017

**Abstract:** This paper presents the free vibration response of piezo laminated composite geometrically nonlinear conical shell panel subjected to a thermo-electrical loading. The temperature field is assumed to be a uniform distribution over the shell surface and through the shell thickness and the electric field is assumed to be the transverse component $E_2$ only. The material properties are assumed to be independent of the temperature and the electric field. The basic formulation is based on higher order shear deformation plate theory (HSDT) with von-Karman nonlinearity. A $C^0$ nonlinear finite element method based on direct iterative approach is outlined and applied to solve nonlinear generalized eigenvalue problem. Parametric studies are carried out to examine the effect of amplitude ratios, stacking sequences, cone angles, piezoelectric layers, applied voltages, circumferential length to thickness ratios, change in temperatures and support boundary conditions on the nonlinear natural frequency of laminated conical shell panels. The present outlined approach has been validated with those available results in the literature.

**Keywords:** Nonlinear free vibration, Laminated composite conical shell panel, $C^0$ nonlinear finite element method

## 1 Introduction

The laminated composite structures are one of the most important structural material due to their superior structural performance with outstanding properties such as high specific strength and stiffness, better corrosion and fatigue resistance, and design flexibility as per requirements. Shell panels are the basic structural element of modern technology. In shell panels, a conical shell panel is being widely used structucture in aerospace application for rocket interstages, satellite carrier adapters for spacecraft launchers, payload fairings (launch vehicle fairings), radomes, spacecraft fittings, missile motor cases, fuselage and fuel tank components for aerial vehicles, etc. During applications, this structure is subjected to very high intensity of thermo-eletro-mechanical loadings. To avoide the resonance free structure, the analysis of nonlinear free vibrations of conical shell panel is nessesary for optimum performence. Aside from this, the analysis of thermal loading is also extremely important for the structural integrity and stability of the structures. Analysis of direct and converse piezoelectric effects is necessary by coupling surface bonded or embedded piezoelectric actuator and/or sensor layers which act as a transducer between electricity and mechanical stress can add an advantage by automating the vibration control.

Certain efforts have been made in the past by researchers for the prediction of structural responses with and without use of thermo-piezo-electro-mechanical loadings on conical shell panels to evaluate the various responses such as buckling, vibration, bending and failure etc. For example: Correia *et al.* [1] carried out the structural analysis of laminated conical shell panels using a quadrilateral isoparametric finite element with the application of higher-order shear deformation theory (HSDT) in which the displacement expressions used for longitudinal and circumferential components of displacement field are given by power series of the transversal coordinate. Patel *et al.* [2] studied the thermoelastic post buckling behavior of cross-ply laminated composite conical shells under uniform temperature distribution in which critical temperature parameter values corresponding to the onset of bifurcation have been compared with linear eigenvalue analysis. A semi-analytical shell finite element model is de-

***Corresponding Author: Achchhe Lal:** S.V. National Institute of Technology Surat-India-395007 Surat, Gujarat India; Email: achchhelal@med.svnit.ac.in
**Niranjan L. Shegokar:** Dr. D.Y. Patil School of Engineering and Technology, Lohgaon, Pune Contact No. 9975140257

veloped with piezoelectric ring actuators/sensors for active damping vibration control of structures using mixed finite element approach by Correia *et al.* [3]. Kulkarni *et al.* [4] presented a finite element formulation for degenerate conical shell element using HSDT with piezoelectric material assuming a parabolic shear strain variation over the thickness. Moita Jose *et al.* [5] developed a finite element formulation based on Kirchhoff classical laminated theory for active vibration control of plate laminated structure with integrated piezoelectric sensors and actuators using Kirchhoff classical laminated theory. Abdullah *et al.* [6] reported the prediction of the buckling and dynamic response of laminated composite structures considering the material properties as deterministic. Bhimaraddy *et al.* [7] developed an isoparametric finite element analysis for laminated shells of revolution by taking into account the effects of shear deformation and rotary inertia. Singh *et al.* [8, 9] developed a finite element method in conjunction with the first order perturbation technique for thermal buckling analysis of laminated composite conical shell panel with and without piezoelectric layers. The theory is developed for nonlinear free vibration of the conical shell [10, 11]. Ganesan *et al.* [12] analyzed the piezoelectric composite cylindrical shells operating in a steady state axisymmetric temperatures using FEM in which the influence of axisymmetric temperature on the natural frequencies and the active damping ratio of the piezoelectric cylindrical shell is also examined. Numerical analysis for free and forced vibration analysis have been carried out for composite conical and cylindrical shells with various approaches [13, 14]. Hu *et al.* [15] developed a methodology for vibration of twisted laminated composite conical shell panels using thin shell theory and the principle of virtual work. Free vibration analysis is carried out for metal and ceramic functionally graded conical shells using first order theory by Zhao *et al.* [16]. Various theories have been developed for the free vibration analysis of plate structures along with the basic theories for composite structures [17–19]. Free vibration of plate structures with or without piezoelectric materials using finite element method based on HSDT with Green Langragian nonlinear strain displacement relation is carried out by Dash. *et al.* [20]. Tripathi *et al.* [21] analyzed the free vibration analysis for a conical shell with random material properties and also obtained natural frequency results for a conical shell by varying geometrical parameters. Sofiyev *et al.* [22] carried out the analytical procedure for the study of free vibration and stability characteristics of homogeneous and nonhomogeneous orthotropic truncated and composite conical shells with clamped edges under uniform external pressures. Chih *et al.* [23] presented a solution of laminated composite conical shells subjected to axisymmetric loads using perturbation method. Korjakin *et al.* [24] carried out the damping analysis for free vibration of laminated composite conical shells using first order shear deformation theory in connection with energy method. Chang *et al.* [25] developed the frequency equations for free vibration of the conical shell with various end conditions but free from the in-plane shearing force along with the asymptotic expressions. Bardell *et al.* [26] carried out a general analysis of the vibration characteristics of thin, open, conical isotropic panels using the h-p version of the finite element method in conjunction with Love's thin shell equations. Lim *et al.* [27] developed a mathematical model for free vibration of shallow composite conical shells in an effort towards accurate modeling of turbomachinery blades in which the study focus is on glass/epoxy conical shells with four and eight ply laminates. A global computational approach based on the external energy principle is employed to derive the eigenvalue equation. Singh *et al.* [28] carried out vibration analysis of composite plates using higher order shear deformation theory and obtained results for fundamental natural frequency of composite plates. Lim *et al.* [29] carried out analysis for vibration behavior of shallow conical shells by global Ritz formulation based on the energy principle. Lal *et al.* [30] examined the second order statistics of nanlinear natural frequency of piezolaminated composite conical shell panel subjected to thermo-electro-mechanical loading using HSDT based on $C^{\circ}$ nonlinear finite combined with SOPT . Lal *et al.* [31] evaluated the second order statistics of post buckling response of laminated piezoeltric composite plate resting on elastic foundation using micromechanical approach in the framework of HSDT in conjunction with SOPT. Chaodhari *et al.* [32] evaluated the statistics of nonlinear fundamental frequency response of elastically supported carbon nanotube-reinforced cvomposite beam with the thermal environment in non-deterministic framework using $C^{\circ}$ nonlinear finite element method combined with second order perturbation method. Zhao *et al.* [33], evaluated the free vibration analysis of conincal shell panels using element free Galerkin's method using classical thin shell theory based on Love's hypothesis. Jooybar *et al.* [34], evaluated the thermally induced free vibration response of functionally graded truncated conical shell panels using the first-order shear deformation theory (FSDT).

It is evident from the available literature that the studies on nonlinear free vibration analysis of piezolaminated composite conical shell panel subjected to thermoelectrical load are rearly dealt by the researchers due to the complexity associated with the conical shell panels. In the present work, an attempt is made to address this prob-

lem by using computationally efficient $C^0$ nonlinear finite method.

The contribution of this paper is to compute the nonlinear natural frequency of piezolaminated composite conical shell panels subjected to thermopiezoeletric loadings using a direct iterative based $C^0$ nonlinear finite element method with HSDT in von-Karman nonlinearity. To implement this theory, a suitable $C^0$ continuous isoparametric finite element method with seven DOFs per node is proposed in order to reduce the computational efforts required in the formulation of element matrices without affecting the solution accuracy. The validation of the present outlined approach is performed by comparing the results with those reported in the literature. Typical results for nonlinear natural frequency of laminated conical shell panel with various ply orientations, layup sequences, and circumferential length to thickness ratios, material properties, piezoelectric layers, thermal load, applied voltages, and boundary conditions have been investigated. The results are presented in the form of tables, which can suit as a benchmark for the future results.

## 2 Formulation

A composite laminated conical shell panel of top radius $R_1$, bottom radius $R_2$, thickness $h$, circumferential length (LC) and half semi-cone angle ($\varphi$) consist of $N$ layer parallel fibers embedded in a matrix with its coordinate definition and material direction of a typical lamina are shown in Figure 1. Let ($\overline{u}_1$, $\overline{u}_2$, $\overline{u}_3$) be the displacements parallel to the coordinate system ($s$, $\theta$, $z$) located on the reference plane ($z$ =0) of the conical panel are shown in Figure 1. It is assumed that a perfect bonding exists between the fibers and the matrix so that no slippage can occur at the interface and the strains experienced by the fiber, matrix, and composite are equal. The fibers are assumed to be

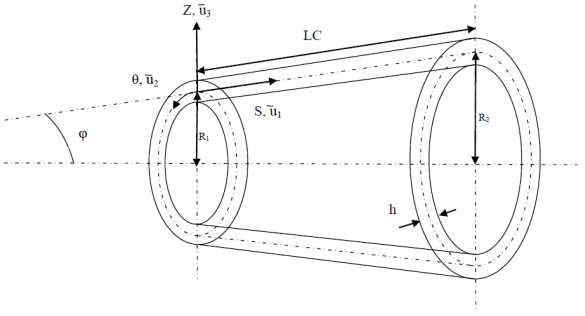


**Figure 1:** Geometry of laminated composite cone lamina with geometrical coordinates

uniform in properties and diameter continues and parallel throughout the composite. It is also assumed that the composite behaves like homogeneous composite material and the effects of the average constituent's materials (*i.e.*, matrix and fiber) are detected combined. All the formulation part is confined here with the assumption of a linear elastic material behavior with large displacement and strains assuming von-Karman type.

The assumed displacement field to model the conical shell panel is based on the higher order shear deformation theory (HSDT) with von-Karman nonlinearity. The condition of zero transverse shear stresses on the top and bottom of the conical shell is imposed to determine the higher order terms on the displacement field. After imposing these conditions, the displacement field as given in [1] for the conical shell/panel is modified and expressed as:

$$\overline{u}_1(s,\ \theta,\ z) = u + \left(z - \frac{4z^3}{3h^2}\right)\beta_s - z^3\frac{4}{3h^2}\frac{\partial w}{\partial s} \tag{1}$$

$$\overline{u}_2(s,\ \theta,\ z) = \left(1 + \frac{z}{R_2}\right)v + \left(z - \frac{4z^3}{3h^2}\right)\beta_\theta - z^3\frac{4}{3h^2}\frac{1}{R_\theta}\frac{\partial w}{\partial \theta}$$

$$\overline{u}_3(s,\ \theta,\ z) = w$$

where $\left(\overline{u}_1,\ \overline{u}_2,\ \overline{u}_3\right)$ are the displacement along $\left(s,\ \theta,\ z\right)$ coordinates and $\left(u,\ v,\ w\right)$ are the displacements of a point on the middle surface with $\beta_s$ and $\beta_\theta$ as the rotations of the normal to the mid-plane about $s$ and $\theta$ direction, respectively and $R_\theta$ is the principal radius of curvature in the $\theta$ direction.

From eq. (1), it can be observed that the expression for in plane displacement $\overline{u}_1$ and $\overline{u}_2$ involve the derivatives of out of plane displacement $w$, as a result of this, second order derivatives would be present in the strain vector, therefore it is the necessity of the implement of $C^1$ continuity. The complexity and difficulty involved with making a choice of $C^1$ continuity (for solving partial differential equations) are well known in order to avoid some difficulties associated with these elements; the displacement field model has been slightly modified to make it suitable for $C^0$ continuous element [19]. The $C^0$ continuous element permits easy isoperimetric finite element formulation and consequently can be applied for nonrectangular geometries as well. Thus five DOFs with $C^1$ continuity given in eq. (1) can be increased to 7 DOFs with $C^0$ continuity due to conformity with HSDT. In this change, the artificial constraints are imposed, which can be enforced variationally through a penalty approach, in order to satisfy the constraint emphasized. However, the literature [19] demonstrated that without enforcing these constrains, accurate results with $C^0$ continuity can be obtained. The displacement model is given in eq. (1) can be written in the modi-

fied form as

$$\bar{u}_1(s,\ \theta,\ z) = u + f_1(z)\beta_s + f_2(z)\theta_s; \quad (2)$$
$$\bar{u}_2(s,\ \theta,\ z) = v\left(1 + \frac{z}{R_2}\right) + f_1(z)\beta_\theta + f_2(z)\theta_\theta;$$
$$\bar{u}_3(s,\ \theta,\ z) = w;$$

where the function $f_1(z)$,$f_2(z)$, $\theta_s$ and $\theta_\theta$ can be defined as

$$f_1(z) = C_1 z - C_2 z^3; \quad f_2(z) = -C_4 z^3; \quad (3)$$
$$\theta_s = \frac{\partial w}{\partial s} \quad \text{and} \quad \theta_\theta = \frac{\partial w}{\partial \theta} \quad \text{with}$$
$$C_1 = 1,\ C_2 = C_4 = \frac{4h^2}{3}$$

The displacement vector for the modified $C^0$ continuous model is denoted as

$$f = \begin{pmatrix} u & v & w & \theta_\theta & \theta_s & \beta_\theta & \beta_s \end{pmatrix} \quad (4)$$

The electric potential generated for the piezoelectric layer is assumed as$\phi$ is electric potential, which can be assumed as

$$\phi(s,\theta,z) = \phi^{(0)}(s,\theta) + z\phi^{(1)}(s,\theta) + z^2\phi^{(2)}(s,\theta) \quad (5)$$

where $\phi^{(0)}$, $\phi^{(1)}$ and $\phi^{(3)}$are the electric potential terms.

The nonlinear coupled piezothermoelectric constitutive equations can be written as of an orthotropic layer/lamina (say $p^{th}$ layer) having any fiber orientation with respect to structural axes system $(s-\theta-z)$ [35]

$$\bar{\sigma}_{ij} = \bar{C}_{ij}^{p}\left(\bar{\varepsilon}_{ij}^{L} + \bar{\varepsilon}_{ij}^{NL} - \bar{\varepsilon}_{ij}^{T} - \bar{\varepsilon}_{ij}^{V}\right) - e_{kl}E_k \quad (6a)$$
$$(i,j = 1,2,\ldots,6 \quad \text{and} \quad k,\ l = 1,2,3)$$

$$D_k = e_{kj}\left(\bar{\varepsilon}_{ij}^{L} + \bar{\varepsilon}_{ij}^{NL}\right) + \xi_{kl}E_l + p_k\Delta T, \quad (6b)$$
$$(i,j = 1,2,\ldots,6 \quad \text{and} \quad k,\ l = 1,2,3)$$

where $\bar{C}_{ij}^{p}$ is the reduced elasticity constants matrix and $\bar{\varepsilon}_{ij}^{L}$, $\bar{\varepsilon}_{ij}^{NL}$, $\bar{\varepsilon}_{ij}^{T}$ are the linear, nonlinear and thermal strain vector, respectively, $e_{kl}$ is the matrix of the piezoelectric coefficients, $E_k$ is the electric field vector, $\Delta T$ is the temperature rise from a stress free reference temperature, $D_k$ is the electric displacement vector, $\xi_{kl}$ is the dielectric coefficient matrix, and $p_k$ is the piezoelectric constants vector. The electrical field $E$ is calculated based on the gradient of the electric potential given in Eq. (5).

From Eq. (6a) linear strain tensor can be rewritten as

$$\bar{\varepsilon}_{ij}^{L} = H_{mn}\varepsilon_{kl}^{L} \quad (7)$$

where $H_{mn}$ is the function of $Z$ and unit step vector defined in the appendix (A.1) and $\varepsilon_{kl}$ is reference plain linear strain tensor defined as

$$\varepsilon_{kl}^{L} = \quad (8)$$

$$\begin{Bmatrix} \varepsilon_1^0 & \varepsilon_2^0 & \varepsilon_6^0 & k_1^0 & k_2^0 & k_6^0 & k_1^2 & k_2^2 & k_6^2 & \varepsilon_4^0 & \varepsilon_5^0 & k_4^2 & k_5^2 \end{Bmatrix}^T$$

Assuming that the strains are much smaller than the rotations (in the von-Karman sense), one can rewrite nonlinear strain vector $\left\{\bar{\varepsilon}_{ij}^{NL}\right\}$ of the Eq. (6a) as [36],

$$\bar{\varepsilon}_{ij}^{NL} = \frac{1}{2}\,[A_{nl}]\,\{\phi\} \quad (9)$$

where $A_{nl} = \frac{1}{2}\begin{bmatrix} w,_s & 0 \\ 0 & w,_\theta \\ w,_\theta & w,_s \\ 0 & 0 \\ 0 & 0 \end{bmatrix}$ and $\phi = \begin{Bmatrix} w,_s \\ w,_\theta \end{Bmatrix}$

The thermal strain vector $\left\{\bar{\varepsilon}_{ij}^{T}\right\}$given in Eq. (6) can be represented as

$$\bar{\varepsilon}_{kll}^{T} = \Delta T \begin{Bmatrix} \alpha_1 \\ \alpha_2 \\ 0 \\ 0 \\ 0 \end{Bmatrix} \quad (9a)$$

where $\alpha_1$ and $\alpha_2$ are thermal expansion coefficients along the $s$, and $\theta$ direction, respectively which can be obtained from the thermal in the longitudinal $(\alpha_l)$ and transverse $(\alpha_t)$ directions of the fibers using transformation matrix and $\Delta T$ is the change in temperature in the shell panel subjected with uniform temperature rise.

The electric field vector$\left\{\bar{\varepsilon}_{ij}^{V}\right\}$given in Eq. (6) can be represented as

$$\bar{\varepsilon}_{kll}^{V} = E_z \begin{Bmatrix} d_{31} \\ d_{32} \\ 0 \\ 0 \\ 0 \end{Bmatrix} = \frac{V_k}{t_k} \begin{Bmatrix} d_{31} \\ d_{32} \\ 0 \\ 0 \\ 0 \end{Bmatrix} \quad (9b)$$

where $d_{31}$ and $d_{32}$ are the piezoelectric strain constant of a single ply along the $s$, and $\theta$ direction respectively which can be obtained from the thermal in the longitudinal and transverse directions of the fibers using transformation matrix and $E_z$, $V_k$, $t_k$ are the electric field along the thickness direction, applied voltage across the $k^{th}$ ply and thickness of the ply in the shell panel subjected with uniform electric field rise.

From Eq. (6a), the electric field vector $E_k$is calculated based on the gradient of the electric potential $\varphi$ can be written as

$$E_k = H_{mn\phi}E_{kl} \quad (10)$$

where $H_{mn\phi}$ is the function of z and unit step vector of piezoelectric layers defined in the appendix (A.2) and $\varepsilon_{kl}^{\phi}$is

reference plain piezoelectric strain tensor defined as

$$E_{kl} = \left\{ E_s^{(0)} \quad E_\theta^{(0)} \quad E_s^{(1)} \quad E_\theta^{(1)} \quad E_s^{(2)} \quad E_\theta^{(2)} \quad X^{(1)} \quad X^{(2)} \right\}^T \tag{10a}$$

with $H_{mn\phi} = \begin{bmatrix} 1 & 0 & z & 0 & z^2 & 0 & 0 & 0 \\ 0 & 1 & 0 & z & 0 & z^2 & 0 & 0 \\ 0 & 0 & 0 & 0 & 0 & 0 & 1 & z \end{bmatrix}$.

where, $E_s$, $E_\theta$, and $X$ are electric field vector along $s$, $\theta$, $z$ direction, respectively, and $H_{mn\phi}$ is the unit step vector of electric field vector.

From Eq. (2) the displacement components at any point within the cone may also be expressed as

$$\overline{u}_i = \left\{ \overline{u}_1 \quad \overline{u}_2 \quad \overline{u}_3 \right\}^T \tag{11a}$$

The Eq. (11a) can be rewritten in general form

$$\overline{u}_i = S_{kl} u_i, \quad \text{with} \quad (k = 1, 2, 3 \text{ and } l = 1, 2, \ldots, 9) \tag{11b}$$

where $u_i$ is the displacement vector of any point in the reference plane and $S_{kl}$ = function of $z$ and unit step functions defined in the appendix (A.3).

The total energy of the system consisting of linear, nonlinear and piezoelectric stain energy of the conical shell panel with work done due to thermal and electrical loading can be expressed as

$$U_S = U_L + U_{NL} - W_T - W_V - U_\phi \tag{12}$$

From Eq. (12) the linear stain energy of the conical shell is given by

$$U_L = \int_\Omega \frac{1}{2} \overline{C}_{ijkl}^p \overline{\varepsilon}_{ij}^L \overline{\varepsilon}_{kl}^L d\Omega = \int_\Delta \frac{1}{2} \varepsilon_{ij} D_{mn} \varepsilon_{kl} d\Delta \tag{13}$$

where $D_{mn}$ is the laminate elastic stiffness matrix defined in the appendix (A.4).

From Eq. (12), the nonlinear strain energy matrix can be rewritten as

$$U_{NL} = \int_\Omega \frac{1}{2} \overline{\varepsilon}_{ij}^{NL} \overline{C}_{ijkl}^p \overline{\varepsilon}_{kl}^{NL} d\Omega = \int_\Delta \frac{1}{2} \varepsilon_{ij}^{NL} D_{ijkl}^{NL} \varepsilon_{kl}^{NL} d\Delta \tag{14a}$$

where $D_{ijkl}^{NL}$ is the laminate stiffness matrices defined in the appendix (A.5).

Using Eq. (9), the Eq. (14a) can be expressed as

$$U_{NL} = \frac{1}{2} \int_\Omega A_{nij} \phi_{nij} D_3 \overline{\varepsilon}_{ij}{}^L d\Omega + \frac{1}{2} \int_\Omega \overline{\varepsilon}_{ij}{}^L D_4 A_{nkl} \phi_{nkl} d\Omega + \frac{1}{2} \int_\Omega A_{nij} \phi_{nij} D_5 A_{nkl} \phi_{nkl} d\Omega, \quad (i, j, k, l = 1, 2, 3) \tag{14b}$$

where $D_3$, $D_4$ and $D_5$ are the laminate stiffness matrices of the conical shell panel defined in appendix (A.6).

From Eq. (12), the work done due to thermal loading can be written as

$$W_T = \int_\Omega \frac{1}{2} B_j N_0^T B_j^T d\Omega = \int_\Delta \frac{1}{2} B_j \lambda_T \overline{N}_0^T B_j^T d\Delta \tag{14c}$$

where $B_j$ is the geometric stiffness matrix defined in appendix (A.7). The parameters $\overline{N}_0^T$ is the thermal compressive stress resultant matrix defined in the appendix (A.8) and $\lambda_T$ is the critical thermal parameter.

From Eq. (12), the work done due to applied electric field can be written as

$$W_V = \int_\Omega \frac{1}{2} B_j^V N_0^V B_j^V d\Omega = \int_\Delta \frac{1}{2} B_j^V \lambda_V \overline{N}_0^V B_j^V d\Delta \tag{14d}$$

where $\overline{N}_0^V$ is the applied electric field stress resultant matrix defined in the appendix (A.9) and $\lambda_V$ is the critical electric field parameter.

From Eq. (12), the strain energy due to piezoelectric layers can be rewritten as

$$U_\phi = U_{\phi L} + U_{\phi NL} \tag{15}$$

From Eq. (15), the linear strain energy due to piezoelectric layers $(U_{\phi L})$ can be rewritten as

$$U_{\phi L} = \int_\Omega \frac{1}{2} \overline{\varepsilon}_{kl}^L D_{1P} \overline{E}_{ij}^\phi d\Omega + \int_\Omega \frac{1}{2} \overline{E}_{kl}^\phi D_{1P}^T \overline{\varepsilon}_{ij}^L d\Omega - \int_\Omega \frac{1}{2} \overline{k}_{ij}^\phi D_{2P} \overline{E}_{ij}^\phi d\Omega \tag{15a}$$

where $D_{1P}$ and $D_{2P}$ are defined in appendix of (A.10) and (A.11), respectively.

The Eq. (15), the nonlinear strain energy due to piezoelectric layers $(U_{\phi NL})$ can be rewritten as

$$U_{\phi NL} = \frac{1}{2} \int \{\phi_p\}^T \{A_{nij}\}^T D_6 \{L_\phi\} \{\phi_{nij}\} ds d\theta + \frac{1}{2} \int \{\phi_{nij}\}^T \{L_\phi\}^T D_7 \{A_{nij}\} \{\phi_p\} ds d\theta \tag{15b}$$

where $D_6$, $D_7$ are the linear piezoelectric stiffness matrices defined in appendix of (A.12).

The kinetic energy of vibrating cone can be expressed as

$$T = \int_\Omega \frac{1}{2} \rho_p \dot{\overline{u}}_i \dot{\overline{u}}_j d\Omega = \int_\Delta \frac{1}{2} M_{jk} \dot{u}_i \dot{u}_j d\Delta \tag{16}$$

where $\rho_p$,$M_{jk}$ are mass density of the $p^{th}$ element and the element consistent mass matrix defined in the appendix (A.13), respectively and the dot indicates derivative with respect to time "$t$."

## 3 Governing equation of motion

The equation of motion for nonlinear free vibration response of the laminated composite cone in thermal environmental can be derived using Hamilton's variational principle

$$\delta \int_{t1}^{t2} (T - U_S) dt = 0 \tag{17}$$

Using Eqs. (13), (14a), (14b), (14c), (14d) and (16) the strain-displacement relation (defined in appendix) in the reference plane, which is derived and expressed as

$$\int_{\Delta} M_{mn} \ddot{u}_{i_1} \delta u_{i_1} + \int_{\Delta} D_{m_1 n_1} u_{i_1, j_1} \delta u_{k_1, l_1} d\Delta = 0 \tag{18}$$

The above eq. (18) can be further written as

$$\int_{\Delta} M_{mn} \ddot{u}_{i1} \delta u_{i1} d\Delta + \int_{\Delta} D_{m_1 n_1} \ddot{u}_{i1} \delta u_{k1,l1} d\Delta = 0 \tag{19}$$

In the present study, a nine-noded quadrilateral $C^0$ isoparametric element with the seven field variables per node ($s$, $\theta$, $z$, $\theta_s$, $\theta_\theta$, $\beta_s$ and $\beta_\theta$) is employed. The generalized field variable ($f$) at any point within the element is expressed in terms of nodal variables as follows:

$$f = \sum_{i=1}^{nn} N_i f_i \tag{20}$$

where $f_i$ is the field variable corresponding to the $i^{th}$ node; $N_i$ is the shape function associated with the $i$th node and $nn$ is the number of nodes per element, which is nine in the present study.

Using the Eq. (20), the strain tensor $\mathcal{E}_{ij}$ and the displacement vector $u_\alpha$ may be expressed in terms of nodal displacement vector $\{\delta\}$ as

$$\varepsilon_{ij} = B_{ij\alpha} \delta_\alpha, \quad u_\alpha = P_{ij\alpha} \delta_\alpha \tag{21}$$

where $B_{ij\alpha}$ is the strain displacement matrix.

Substituting the above finite element approximations of Eq. (20) into Eq. (19), the finite-element equations of motion are obtained as

$$M_{\alpha\beta}(b_\rho) \ddot{\delta}_\beta(b_\rho) + K_{\alpha\beta}(b_\rho) \delta_\beta(b_\rho) = 0 \tag{22}$$

In the above equation, $M_{\alpha\beta}(b_\rho)$ and $K_{\alpha\beta}(b_\rho)$ are the mass and stiffness tensor.

The finite element equations of motion, [Eq. (22)] may be further written with the help of a trial function $\delta_\beta(b_\rho; t) = q_\beta(b_\rho) \exp[i(t - t_0)]$ in the form of standard eigen-value problem for free vibration analysis having one system of n static equations (time is assumed as deterministic) can be expressed as:

$$[K_{\alpha\beta}(b_\rho) - \lambda_\beta(b_\rho) M_{\alpha\beta}(b_\rho)] q_\beta(b_\rho) = 0 \tag{23}$$

where $K_{\alpha\beta} = [K_{l\alpha\beta} + K_{nl\alpha\beta} - K_{g\alpha\beta} - K_{V\alpha\beta} - K_{q\alpha\beta\phi} K^{-1}_{\alpha\beta\phi} K_{q\alpha\beta\phi}]$ with $K_{nl\alpha\beta} = [\frac{1}{2} N_1(\delta_\beta) + \frac{1}{3} N_2(\delta_\beta)]$
where $q_\beta$, $K_{l\alpha\beta}$, $K_{nl\alpha\beta}$, $K_{g\alpha\beta}$,$K_{V\alpha\beta}$,$K_{q\alpha\beta\phi}$, $K_{\alpha\beta\phi}$, $M_{\alpha\beta}$ and $\lambda_\beta\ (= \omega^2)$ are defined as global (system) eigen vector, linear, nonlinear, geometric stiffness (arises due to thermo-electrical loadings) matrices, elective field stiffness, coupling matrix between elastic mechanical and electrical effects, dielectric stiffness matrix, mass matrix and system eigenvalue, respectively [30]. The parameters $[N_1(\delta_\beta)]$ and $[N_2(\delta_\beta)]$ are global nonlinear stiffness matrices which are linearly and quadratically dependent on the displacement vector, respectively [33].

Eq. (23) involve only mean quantities and is a deterministic eigen value equation from which the mean eigen value of vibration frequencies can be obtained by solving the zeroth-order eigenpairs $\lambda_\beta(b_\rho)$ and $q_\beta(b_\rho)$ by any conventional technique. Since $\lambda^\rho_\beta$ is diagonal and $K_{\alpha\beta}$ and $M_{\alpha\beta}$ are symmetric, the first term on the left hand side of the above equation vanishes by the use of Eq. (23).

The nonlinear eigenvalue problem as given in Eq. (23) is solved by employing a direct iterative method based on $C^0$ nonlinear finite element with the following steps

- Step 1: By setting amplitude to zero, the linear eigenvalue problem $[K_{\alpha\beta} q_\beta = \lambda_\beta M_{\alpha\beta} q_\beta, \quad \lambda_\beta = {\omega_{ij}}^2]$ is obtained from Eq. (22) with all nonlinear terms set to zero, by assuming that the system vibrates in its principal mode to obtain the linear eigen value and eigen vector.
- Step 2: The mean mode shape of the desired linear mode is normalized with respect to given amplitude at the point of maximum deflection.
- Step 3: Using the normalized mode shape, the nonlinear stiffness matrix is computed with this initial displacement.
- Step 4: By applying these stiffness matrices the eigenvalue problem is then solved to obtain new eigenvalue and corresponding eigenvectors.
- Step 5: Steps (2) to (4) are repeated until convergence ($\leq 10^{-2}$) is attained for maximum displacement $\{\delta_\beta\}_{\max}$and the corresponding mean natural frequency $\left(\omega_{ij} = \sqrt{\lambda_\beta}\right)$ is computed.

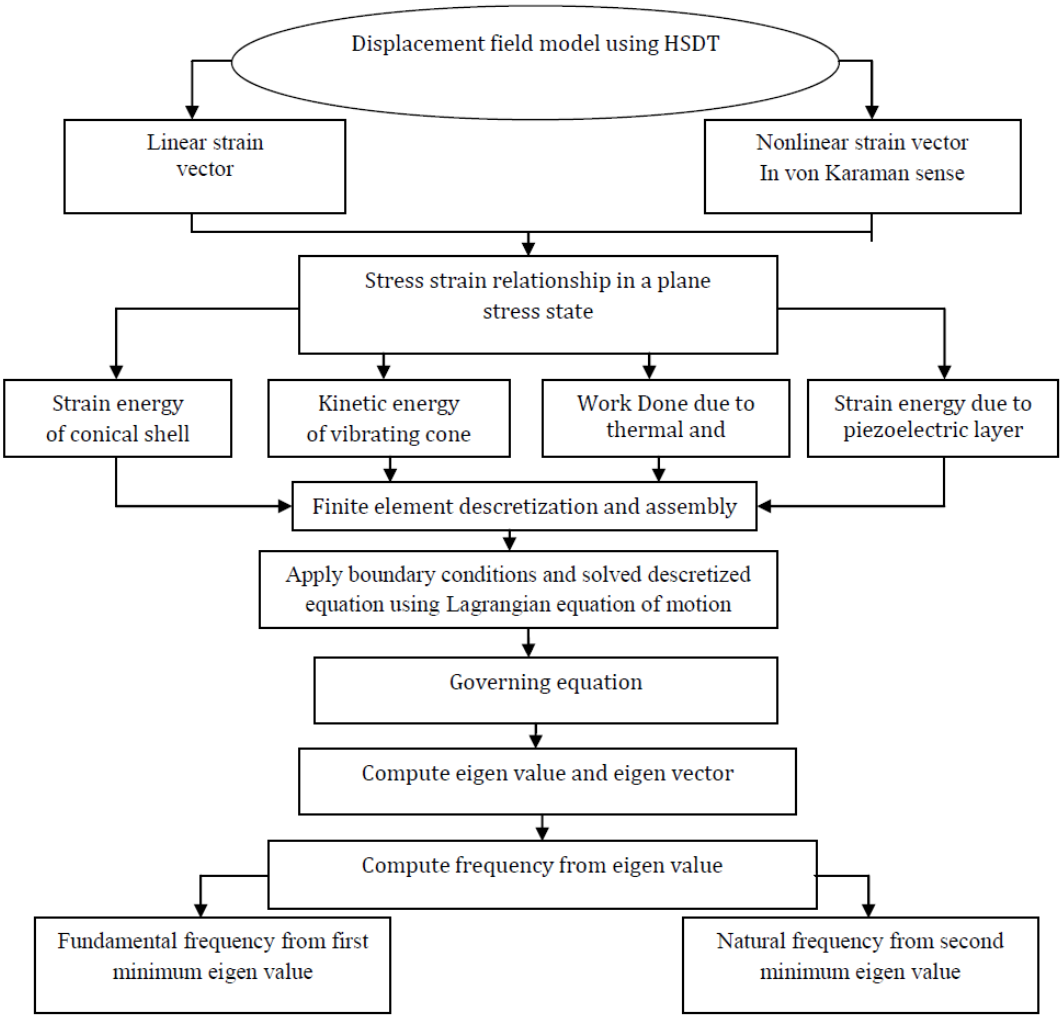


**Figure 2:** Flow chart for an overview of the present analysis

## 4 Results and Discussion

The direct iterative based $C^0$ nonlinear finite element method outlined for nonlinear free vibration is applied and illustrated for different boundary conditions, piezoelectric layers, circumferential length to curvature ratios, amplitude ratios, lamination schemes, cone thickness ratios and thermal and electrical loading. A nine noded Lagrangian isoparamatric element, with 63 degrees of freedom (DOFs) per element for the present HSDT model has been used for discretizing the laminate. Based on convergence study conducted a (4 × 4) mesh has been used throughout the study. A computer program has been developed in MATLAB R2009a environment to generate the numerical results. It is noted that for the computation of results full integration (3 × 3) is used for thick shells and selective integration scheme (2 × 2) for the thin shell. In the present analysis, various parameters such as circumferential length to thickness ratios, amplitude ratios, and boundary conditions are used to check the efficiency of the present model. However, present outlined formulation, solution technique, and code do not put any limitations. It is assumed that the materials are perfectly elastic throughout the deformation.

The following dimensionless quantity and ratio has been used in this study, $\overline{\omega} = (\omega a^2\sqrt{\rho/E_2})/h$, where, $\overline{\omega}$, $\omega$, $\rho$, $a$, $E_2$ and $h$ are defined in notation.

The ratio of nonlinear to linear frequency = $\overline{\omega}_{nl}/\overline{\omega}_l$

In the present study, various combinations of boundary edge support conditions (BCs) namely clamped, simply supported (S1 and S2) and clamped simply supported boundary condition for conical shell panel has been used for the present analysis.

(a) All edges simply supported (SSSS) (S1):

$$u = v = w = \theta_\theta = \beta_\theta = 0, \text{ at } s = 0,\ a;$$
$$u = v = w = \theta_s = \beta_s = 0 \text{ at } \theta = 0,\ b;$$

(b) All edges simply supported (SSSS) (S2):

$$v = w = \theta_\theta = \beta_\theta = 0, \text{ at } s = 0,\ a;$$
$$u = w = \theta_s = \beta_s = 0 \text{ at } \theta = 0,\ b;$$

(c) All edges clamped (CCCC):

$$u = v = w = \beta_s = \beta_\theta = \theta_s = \theta_\theta = 0,\ at\ s = 0,\ a$$
$$\text{and } \theta = 0,\ b;$$

(d) Two opposite edges clamped and other two simply supported (CSCS):

$$u = v = w = \beta_s = \beta_\theta = \theta_s = \theta_\theta = 0,\ at\ s = 0$$
$$\text{and } \theta = 0; v = w = \theta_\theta = \beta_\theta = 0,$$
$$\text{at } s = a\ \ u = w = \theta_s = \beta_s = 0, \text{ at } \theta = b;$$

Material properties for composite and piezoceramic are as shown in Table 1 and Table 2.

**Table 1:** The following elastic properties of materials used for computation of numerical results

| Elastic properties | Graphite/Epoxy (Mean values) | | Piezoceramic |
|---|---|---|---|
| | Material 1 | Material 2 | |
| $E_1$ (GPa) | 40 $E_2$ | 25 $E_2$ | 63 |
| $E_2$ (GPa) | 6.92 | 10.3 | 63 |
| $G_{12}$ (GPa) | 0.6 $E_2$ | 0.5 $E_2$ | 24.2 |
| $G_{13}$ (GPa) | 0.6 $E_2$ | 0.5 $E_2$ | 24.2 |
| $G_{23}$ (GPa) | 0.5 $E_2$ | 0.2 $E_2$ | 19 |
| $\nu_{12}$ | 0.25 | 0.25 | 0.3 |
| $\alpha_1(10^{-6})$ | 1.1 | 1.1 | 0.9 |
| $\alpha_2(10^{-6})$ | 25.2 | 25.2 | 0.9 |

## 4.1 Validation Study

In order to ensure the accuracy and proficiency of present outlined direct iterative based $C^0$ nonlinear finite element method, three sets of examples have been analyzed for free vibration of conical shell panel.

**Example 1.** To make certain accuracy of the present finite element formulation, a convergence study for mean natural frequencies for a $[-45°/45°]_S$ laminated composite simply supported cylindrical panel with thickness ra-

**Table 2:** The following piezoelectric properties are used for computation of numerical results

| Piezoelectric properties | Graphite/Epoxy Material 1 | Graphite/Epoxy Material 2 | Piezoceramic |
|---|---|---|---|
| Piezoelectric coefficients ($10^{-12}$ m/V) | | | |
| $d_{32}$ | 0 | 0 | −285 |
| $d_{24}$ | 0 | 0 | 122 |
| $d_{15}$ | 0 | 0 | 122 |
| Electric permittivity ($10^{-11}$ F/m) | | | |
| $e_{11}$ | 0 | 0 | 1475 |
| $e_{22}$ | 0 | 0 | 1475 |
| $e_{33}$ | 0 | 0 | 1300 |

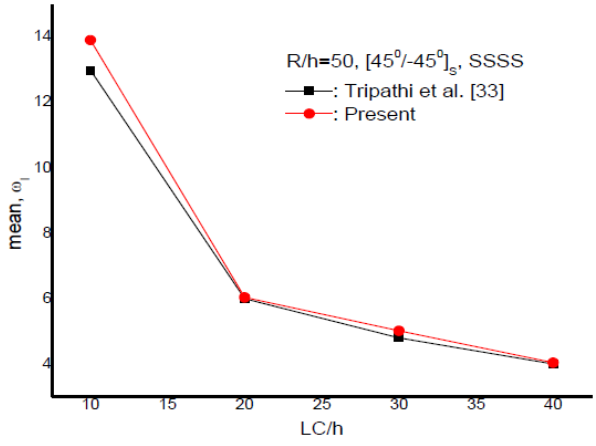


**Figure 3:** Validation study of mean fundamental frequency in 1000 rad/s for a laminated $[-45°/45°]_s$ simply supported cylindrical panel, with R/h=50, for the discrete value of LC/h

**Table 3:** Validation study of fundamental frequency for simply supported (S2) conical shell panel with $\varphi_s = 10°$, $LC/h = 1000$

| $W_{max}/h$ | Lim *et al.* [29] | Present |
|---|---|---|
| 0.2 | 239.15 | 240.25 |
| 0.3 | 358.72 | 360.02 |
| 0.4 | 478.31 | 479.58 |
| 0.5 | 597.90 | 599.81 |
| 0.6 | 717.49 | 719.30 |
| 0.7 | 837.10 | 840.22 |
| 0.8 | 956.86 | 959.28 |

**Table 4:** Validation study of dimensionless mean nonlinear fundamental frequency of piezo laminated layers [P/0°/90°/90°/0°] simply supported (S2) plate.

| Mesh | $\omega_l$ | $Wmax/h$ | | | | |
|---|---|---|---|---|---|---|
| | | 0.2 | 0.4 | 0.6 | 0.8 | 1.0 |
| 2 × 2 | 26.132* | 1.020* | 1.0840* | 1.168* | 1.300* | 1.4360* |
| | 25.7380^ | 1.018^ | 1.0712^ | 1.1505^ | 1.2482^ | 1.3576^ |
| 4 × 4 | 25.216* | 1.017* | 1.065* | 1.142* | 1.240* | 1.358* |
| | 25.2378^ | 1.0175^ | 1.0672^ | 1.1430^ | 1.2381^ | 1.3468^ |
| 6 × 6 | 25.150* | 1.015* | 1.060* | 1.136* | 1.256* | 1.339* |
| | 25.211^ | 1.0175^ | 1.0672^ | 1.1427^ | 1.2374^ | 1.3386^ |

^Present , *Dash *et al.* [20]

**Table 5:** Effect of amplitude ratio, frequency mode and stacking sequence on dimensionless mean nonlinear natural frequency of the conical shell panel.

| $Wmax/h$ | Mode | [$0^0$/P/90°/ 90°/0°] | [0°/P/90°/ 0°/90°] |
|---|---|---|---|
| 0.2 | 1 | 22.4509 | 21.0043 |
| | 2 | 37.6789 | 32.2293 |
| 0.4 | 1 | 24.3101 | 22.5487 |
| | 2 | 37.6769 | 33.5145 |
| 0.6 | 1 | 27.0088 | 24.9557 |
| | 2 | 37.6754 | 35.4729 |
| 0.8 | 1 | 30.3130 | 26.7281 |
| | 2 | 37.6814 | 35.6789 |
| 1.0 | 1 | 34.0033 | 27.5572 |
| | 2 | 37.7275 | 35.6719 |

**Table 6:** Effect of amplitude ratio, frequency mode and curvature to thickness ratio on dimensionless mean nonlinear natural frequency with [P/0°/90°/90°/0°] conical shell panel.

| $Wmax/h$ | Mode | $LC/h = 10$ | $LC/h = 20$ | $LC/h = 30$ |
|---|---|---|---|---|
| 0.2 | 1 | 23.5572 | 28.4710 | 29.9226 |
| | 2 | 34.5792 | 70.0617 | 85.3959 |
| 0.4 | 1 | 25.8885 | 30.0880 | 31.4965 |
| | 2 | 34.5797 | 70.0707 | 86.7343 |
| 0.6 | 1 | 28.3988 | 32.4739 | 33.8323 |
| | 2 | 34.5792 | 70.0742 | 88.7733 |
| 0.8 | 1 | 31.4248 | 35.3807 | 36.7321 |
| | 2 | 34.5877 | 69.5659 | 91.3778 |
| 1.0 | 1 | 34.2955 | 38.7386 | 40.1015 |
| | 2 | 35.5611 | 70.0652 | 94.5613 |

tio $R/h = 50$ and circumferential length to thickness ratio $LC/h = 10$ to 40, is carried out as shown in Figure 3 and compared with the available finite element of Tripathi *et al.* [21]. It can be seen that present results obtained by $C^0$ continuity are good arguments with the published results.

**Example 2.** In this example, the dimensionless nonlinear fundamental frequency of conical shell panel with different amplitude ratios is presented and compared with the Ritz method formulation of Lim *et al.* [29] as shown in Table 3. From the table, it can be observed that the present results obtained by $C^\circ$ finite element method with a von-Karman theory for conical shell panel are in good agreement with the available global Ritz method of Lim *et al.* [29].

**Example 3.** In this example, the dimensionless nonlinear fundamental frequency of piezolaminated composite plate with different amplitude ratios and mesh densities are compared and converged with HSDT based finite element results of Dash *et al.* [20] due to unavailability of literature available on free vibration of conical shell panel with piezoelectric layer. The results are presented in Table 4. From the numerical results, it is seen that the present results obtained by $C^0$ FEM with von-Karman nonlinearity are in good agreement with the available results of $C^0$ nonlinear FEM with Green langrage nonlinear strain displacement relations of Dash *et al.* [20]. It is also seen that among the given different mesh sizes such as (2x2), 4x4) and (6x6), the results at (4x4) mesh size has been converged and validated with with the available literature [20]. Hence for the further computation of results, total 16 elements with 7 degree of freedoms have been used. The results are presented in table forms for accuracy point of view and some results are presented with various new parameters which clearly emphasis the importance of these parameters on the natural frequency response of the conical shell panel.

**Table 7:** Effect of lamination scheme, amplitude ratio and frequency mode with position of piezoelectric layer on the dimensionless mean nonlinear natural frequency of conical shell panel.

| Stacking Sequence | $Wmax/h$ | Mode | $P=0$ | $P=1$ | $P=2$ | $P=3$ |
|---|---|---|---|---|---|---|
| $0^\circ/90^\circ/90^\circ/0^\circ$ | 0.5 | 1 | 23.3364 | 27.0549 | 25.5697 | 25.4630 |
| | | 2 | 32.6378 | 34.5787 | 37.6754 | 39.9661 |
| | 1 | 1 | 30.8397 | 34.2955 | 34.0033 | 33.4689 |
| | | 2 | 32.6329 | 35.5611 | 37.7275 | 39.9471 |
| $0^\circ/90^\circ/0^\circ/90^\circ$ | 0.5 | 1 | 21.9177 | 23.1747 | 23.6314 | 25.2234 |
| | | 2 | 32.3743 | 33.1130 | 34.4173 | 38.6117 |
| | 1 | 1 | 27.1924 | 30.2770 | 27.5572 | 31.7095 |
| | | 2 | 32.3716 | 33.0965 | 35.6719 | 38.5862 |
| $0^\circ/90^\circ/0^\circ$ | 0.5 | 1 | 21.9207 | 25.9542 | 24.8965 | 25.9286 |
| | | 2 | 34.5519 | 37.3952 | 37.5787 | 39.8443 |
| | 1 | 1 | 28.9992 | 34.0509 | 29.3401 | 33.7100 |
| | | 2 | 33.5462 | 37.3997 | 39.8057 | 39.8574 |
| $0^\circ/45^\circ/45^\circ/0^\circ$ | 0.5 | 1 | 21.7008 | 24.0790 | 24.1798 | 24.0605 |
| | | 2 | 38.085 | 40.4448 | 38.6779 | 48.8327 |
| | 1 | 1 | 28.2865 | 30.1577 | 30.9125 | 30.9988 |
| | | 2 | 43.8710 | 40.6904 | 42.9175 | 50.9305 |

## 4.2 Numerical Examples for nonlinear natural frequency

The results of thermoelectrically induced natural frequency of laminated conical shell panels are obtained at various parameters such as symmetric and asymmetric cross-ply and /or angle-ply orientation, various boundary conditions (SSSS (S1), (S2), CCCC and CSCS), different circumferential length to thickness ratio ($LC/h$), different amplitude ratio ($W_{max}/h$), semi cone angle ($\varphi$) and material properties etc.

The following parameters are used for computation of results unless otherwise mentioned as $\varphi = 27^\circ$, $LC/h = 10$, $\Delta T = 100, \Delta V = 100$, material number 2 (mentioned in properties table) and SSSS (S2) supported boundary condition.

Table 5 presents the effect of amplitude ratio, frequency mode and stacking sequence on the nonlinear natural frequency of piezolaminated conical shell panel subjected to thermo electrical loading. It is observed that for the same frequency mode and piezo laminated layer, the mean dimensionless frequency increases with the increase of the amplitude ratio. It is also observed that higher frequency mode makes the dimensionless natural frequency higher. Moreover, for the same amplitude ratio and frequency mode, the symmetric cross-ply piezolaminated conical shell panel shows the higher natural frequency.

The effect of amplitude ratio with curvature to thickness ratio on the dimensionless natural mean natural frequency of conical piezolaminated simply supported conical shell panel is examined in Table 6. From the table, it is observed that for the same amplitude ratio and frequency mode, the dimensionless mean natural frequency increases with increase the curvature to thickness ratio. It is because of as the thickness ratio of the panel increases the panel thickness reduces causing it to increase natural frequency. It is also observed that at the same curvature to thickness ratio, the natural frequency of laminated conical shell increases with increase in amplitude ratio and frequency mode.

The effect of the position of a piezoelectric layer with different lamination scheme, for various amplitude ratio and frequency mode and piezolaminated composite conical shell panel, is examined in Table 7. It is observed that for the same lamination scheme and amplitude ratio, the nonlinear mean dimensionless fundamental frequency is higher for 4 layer cross-ply laminates having piezoelectric layer position 1, while, lowest for 4 layers antisymmetric cross-ply shell having piezoelectric layer position 1. It is true for piezoelectric layers at position 2 and 3. Among the three positions of piezoelectric layer ($P$) as given in table are considered as for example cross-ply ($0^\circ/90^\circ/90^\circ/0^\circ$) laminated shell panel, then the $P = 1$ indicates the piezoelectric layer is present at position number 1 as ($P$/0/90/90/0), similarly for $P = 2$, the lamination scheme will be as ($0^\circ/P/90^\circ/90^\circ/0^\circ$) and for $P = 3$, the lamination scheme will be ($0^\circ/90^\circ/P/90^\circ/0^\circ$).

**Table 8:** Effect of material property, amplitude ratio, frequency mode, curvature to thickness ratio and lamination scheme on dimensionless mean nonlinear natural frequency of conical shell panel (LS1 and LS2 indicate [P/0°/45°/0°/45°] and [0°/P/45°/0°/45°], respectively).

| Material type | $Wmax/h$ | Mode | $LC/h = 10$ | | $LC/h = 20$ | |
|---|---|---|---|---|---|---|
| | | | LS1 | LS2 | LS1 | LS2 |
| Material 1 | 0.5 | 1 | 19.3156 | 22.6389 | 21.1362 | 24.4168 |
| | | 2 | 32.1832 | 30.9431 | 38.0529 | 34.7426 |
| | 1 | 1 | 26.2088 | 25.8259 | 28.5291 | 29.0459 |
| | | 2 | 37.3426 | 33.6544 | 47.2453 | 42.7706 |
| Material 2 | 0.5 | 1 | 20.6645 | 23.6314 | 22.7352 | 25.3607 |
| | | 2 | 36.1912 | 34.4173 | 42.6222 | 38.3145 |
| | 1 | 1 | 27.6700 | 27.5572 | 30.1847 | 30.7421 |
| | | 2 | 37.8814 | 35.6719 | 49.5656 | 46.4042 |

**Table 9:** Effect of boundary condition, amplitude ratio, frequency mode and curvature to thickness ratio on dimensionless mean nonlinear natural frequency of conical shell panel with (0°/P/90°/90°/0°) lamination scheme.

| Boundary Condition | $Wmax/h$ | Mode | $LC/h$ | | |
|---|---|---|---|---|---|
| | | | 10 | 20 | 30 |
| SSSS(S1) | 0.5 | 1 | 26.9963 | 30.7637 | 32.1576 |
| | | 2 | 44.9781 | 56.9279 | 61.9514 |
| | 1 | 1 | 33.7481 | 39.4333 | 40.6934 |
| | | 2 | 51.8944 | 61.9560 | 66.7043 |
| SSSS(S2) | 0.5 | 1 | 26.1186 | 30.0053 | 31.3927 |
| | | 2 | 34.4804 | 66.8411 | 61.7915 |
| | 1 | 1 | 32.9291 | 36.4504 | 37.7220 |
| | | 2 | 34.5626 | 61.6607 | 66.4171 |
| CCCC | 0.5 | 1 | 36.2719 | 49.9069 | 56.4387 |
| | | 2 | 55.2608 | 85.9538 | 108.3913 |
| | 1 | 1 | 43.1235 | 55.6653 | 62.1605 |
| | | 2 | 59.2262 | 88.1698 | 110.3838 |
| CSCS | 0.5 | 1 | 30.7802 | 39.3551 | 43.0643 |
| | | 2 | 50.6728 | 73.7474 | 89.4079 |
| | 1 | 1 | 36.7601 | 44.9786 | 48.8022 |
| | | 2 | 55.2943 | 77.2015 | 92.6701 |

Table 8 examines the effect of the material properties with amplitude ratio, frequency mode, curvature to thickness ratio and lamination scheme on the dimensionless mean nonlinear natural frequency of piezolaminated composite conical shell panel in the thermal environment. For the same amplitude ratio, frequency mode and the piezoelectric layer, the mean natural frequency increases for the moderately deep conical shell. It is also observed that the mean fundamental frequency increases and corresponding natural frequency increases as the piezoelectric layer move from the first layer to the second layer. It is due to fact that the piezoletric layeres behaves as senser. Moreover, nonlinear natural frequency higher for the shell panel made of material number 2. It is due to the higher elastic stiffness as compared to material 1.

The effect of support conditions (namely, SSSS (S1), SSSS (S2), CCCC and CSCS), amplitude ratio, frequency mode and curvature to thickness ratio of the nonlinear natural frequency of piezolaminated composite conical shell panel is examined in Table 9. From the table, it is observed that for the same amplitude ratio and curvature to thickness ratio the nonlinear frequency of CCCC shell panel is highest, while SSSS (S2) shows the least numerical and it is true for all other amplitude ratios. It is due to increased effect of boundary constrains of CCCC shell panel is more as compared to other supported shell panel.

**Table 10:** Effect of cone angle, amplitude ratio, frequency mode and stacking sequence on dimensionless mean nonlinear natural frequency of conical shell panel.

| Cone angle | $Wmax/h$ | Mode | P/0°/90°/90°/0° | P/0°/45°/45°/0° |
|---|---|---|---|---|
| 10 | 0.5 | 1 | 14.0369 | 15.2672 |
| | | 2 | 21.1040 | 22.3057 |
| | 1 | 1 | 17.3421 | 19.3582 |
| | | 2 | 23.0902 | 23.7264 |
| 20 | 0.5 | 1 | 24.0160 | 22.1228 |
| | | 2 | 55.5419 | 43.5549 |
| | 1 | 1 | 29.3227 | 26.9011 |
| | | 2 | 59.9157 | 46.9443 |
| 30 | 0.5 | 1 | 45.2054 | 34.7911 |
| | | 2 | 127.732 | 84.4448 |
| | 1 | 1 | 54.1909 | 41.7430 |
| | | 2 | 136.177 | 94.6468 |

**Table 11:** Effect of electrical loading, amplitude ratio, frequency mode, material properties and lamination scheme on dimensionless mean nonlinear natural frequency of conical shell panel with $LC/h = 100$.

| Electric loadings in Volts | $Wmax/h$ | Mode | Material - 1 | | Material - 2 | |
|---|---|---|---|---|---|---|
| | | | P/$[(0°/90°)_2]_S$ | [0°/P/90°/0°/90°] | P/$[(0°/90°)_2]_S$ | [0°/P/90°/0°/90°] |
| 200 | 0.5 | 1 | 34.6449 | 26.8264 | 35.4554 | 27.9351 |
| | | 2 | 96.0435 | 63.9284 | 97.5091 | 67.0797 |
| | 1 | 1 | 38.5651 | 32.0268 | 39.5205 | 33.2173 |
| | | 2 | 101.1452 | 69.8958 | 102.6505 | 73.0737 |
| 0 | 0.5 | 1 | 34.6594 | 26.8655 | 35.4629 | 27.9752 |
| | | 2 | 96.0685 | 63.9730 | 97.5352 | 67.1264 |
| | 1 | 1 | 38.5787 | 32.0308 | 39.5345 | 33.2504 |
| | | 2 | 101.1703 | 69.9970 | 102.6761 | 73.1168 |
| −200 | 0.5 | 1 | 34.6739 | 26.9035 | 35.4849 | 28.0133 |
| | | 2 | 96.0931 | 64.0161 | 97.5597 | 67.1710 |
| | 1 | 1 | 38.5917 | 32.0619 | 39.5481 | 33.2825 |
| | | 2 | 101.1939 | 70.0361 | 102.7006 | 73.1579 |

Table 10 examines the effect of semi cone angle, amplitude ratio, frequency mode with lamination sequence on the mean nonlinear natural frequency of piezolaminated simply supported conical shell panel. It is observed that the nonlinear natural frequency increases with increase in semi cone angle. When the semi cone angle increases, the structures became more conical and the nonlinear natural frequency increases. It is noted that if the height of the conical shell panel is taken as a constant parameter then the nonlinear frequency of conical shell panel increases with increase in semi cone angle.

The effect of electrical loading, amplitude ratio, frequency mode, material properties and piezolamination scheme are examined in Table 11. It is noticed that for same amplitude ratio, frequency mode, and material property, the nonlinear natural frequency decreases with increase in the electrical loading. It is due to that electrical loading makes stiffness of the conical shell lower. The nonlinear frequency of shell panel made of material 2 is higher than material 1. It is because of the stiffness of material 2 are higher.

Table 12 examines the effect of thermal loading, amplitude ratio, frequency mode, material properties and lamination scheme on the dimensionless mean nonlinear natural frequency of piezolaminated conical shell panel. It is noticed that for same amplitude ratio, frequency mode, and material property, the temperature increment makes the frequency lower. It is due to that temperature incre-

**Table 12:** Effect of thermal loading, amplitude ratio, frequency mode, material properties and lamination scheme on dimensionless mean nonlinear natural frequency of conical shell panel with $LC/h = 100$.

| $\Delta$T | $Wmax/h$ | Mode | Material - 1 | | Material - 2 | |
|---|---|---|---|---|---|---|
| | | | P/[(0°/90°)$_2$]$_S$ | [0°/P/90°/0°/90°] | P/[(0°/90°)$_2$]$_S$ | [0°/P/90°/0°/90°] |
| −100 | 0.5 | 1 | 38.9912 | 34.2584 | 39.9621 | 35.3271 |
| | | 2 | 99.9567 | 68.9043 | 101.5106 | 72.1083 |
| | 1 | 1 | 42.6012 | 38.5170 | 43.7095 | 39.7130 |
| | | 2 | 104.8500 | 74.4336 | 106.4429 | 77.6356 |
| 0 | 0.5 | 1 | 36.9396 | 30.9451 | 37.8413 | 32.0173 |
| | | 2 | 98.0279 | 66.3705 | 99.5372 | 69.5589 |
| | 1 | 1 | 40.6704 | 35.4960 | 41.7065 | 36.1436 |
| | | 2 | 103.0490 | 72.1444 | 104.5973 | 75.3213 |
| 100 | 0.5 | 1 | 34.6524 | 26.8464 | 35.4629 | 27.9557 |
| | | 2 | 96.0560 | 63.9509 | 97.5222 | 67.1033 |
| | 1 | 1 | 38.5716 | 32.0148 | 39.5275 | 33.2338 |
| | | 2 | 101.1578 | 69.9770 | 102.6635 | 73.0952 |

ment makes the stiffness of conical shell panel lower. It is also observed that nonlinear frequency of panel is more sensitive to frequency mode 1. It can also be seen that the effect of thermal loading is more dominated as compared to the electrical loading.

# 5 Conclusions

A direct iterative based $C^0$ nonlinear finite element method has been used to obtain the nonlinear natural frequency of piezolaminated composite conical shell panel subjected to uniform thermo-electrical loading acting simultaneously or individually. The following conclusions are noted from the typical results.

1. The nonlinear natural frequency of conical shell panel increases with increase in length to curvature ratios.
2. With increase the amplitude ratio and frequency mode, the nonlinear natural frequency increases.
3. The nonlinear natural frequency of conical shell panel increases with piezoelectric layers and further increases with increasing the piezoelectric layers from the inner side to outer side of the cone from the neutral axis.
4. All edges clamped supported conical shell panel shows higher nonlinear natural frequency as compared to simply supported and clamped and simply supported.
5. Increasing the number of layers initially increases the nonlinear natural frequency but later it becomes constant for a particular circumferential length to thickness ratios.
6. The natural frequency of conical shell panel increases with increase the semi cone angle.
7. There is declination of the nonlinear natural frequency of conical shell panel subjected to thermo-electrical loading acting simultaneously or individually.

# Notations

| | |
|---|---|
| $(A1_{ij}, B_{ij}, D1_{ij}, E_{ij}, F1_{ij}, H_{ij})$ $(A2_{ij}, D2_{ij}, F2_{ij})$ | Laminated plate stiffnesses |
| $\left(M_{1_{ij}}, N_{1_{ij}}, P_{1_{ij}}, Q_{1_{ij}}, R_{1_{ij}}\right)$ $\left(M_{2_{ij}}, N_{2_{ij}}, P_{2_{ij}}, Q_{2_{ij}}, R_{2_{ij}}\right)$ | Piezoeletric layer stiffnesses |
| $\alpha_1, \alpha_2$ | Thermal expansion coefficients along s and $\theta$ direction, respectively |
| $\beta_s, \beta_\theta$ | Rotations of normal to mid plane about the s and $\theta$ axis respectively |
| $\Delta T$ | Difference in temperatures |
| $\omega, \overline{\omega}$ | Fundamental frequency and its dimensionless form |
| $\overline{\sigma_{ij}}, \overline{\varepsilon}_{ij}$ | Stress vector, Strain vector |
| $\overline{C_{ijkl}}^p$ | Reduced elastic material constants |
| $\rho, \lambda$ | Mass density, eigenvalue |
| $\theta_s, \theta_\theta, \theta_k$ | Two slopes and angle of fiber orientation wrt x-axis for kth layer |

| | |
|---|---|
| $E_{11}, E_{22}$ | Longitudinal and Transverse elastic moduli |
| $f, \{f\}^{(e)}$ | Vector of unknown displacements, displacement vector of eth element |
| $G_{12}, G_{13}, G_{23}$ | Shear moduli |
| $N_i$ | Shape function of ith node |
| $\overline{u}_1, \overline{u}_2, \overline{u}_3$ | Displacement of a point $(s, \theta, z)$ |
| $M_{\alpha\beta}, m_{\alpha\beta}$ | Mass and inertia matrices |
| $a$ | Mean radius of conical shell |
| $D$ | Elastic stiffness matrices |
| $ne, n$ | Number of elements, number of layers in the laminated cone |
| $nn$ | Number of nodes per element |
| $u, v, w$ | Displacements of a point on the mid plane of plate |

# References


[1] Pinto Correia I.F., Mota Soares C.M., Mota Soares C.A., Herskovits J. Analysis of laminated conical shell structures using higher order models, Composite Structures, 2003, 62(3–4), 383–390.

[2] Patel B. P., Shukla K. K., and Nath Y., Thermal postbuckling of laminated cross-ply truncated circular conical shell, Composite Structures 2005, 71(1), 101–114.

[3] Pinto Correia I.F, Mota Soares C.M, Mota Soares C.A., Herskovits J. Active control of axisymmetric shells with piezoelectric layers: a mixed laminated theory with a high order displacement field, Computers & Structures, 2002, 80(27–30), 2265–2275.

[4] Sudhakar Kulkarni A., Kamal Bajoria M., Finite element modeling of smart plates/shells using higher order shear deformation theory. Composite Structures, 2003, 62(1), 41–50.

[5] Moita Jose S., Isidoro Correia F.P., Cristovao Mota Soares M, Carlos Mota Soares A., active control of adaptive laminated structures with bonded piezoelectric sensors and actuators, Computers & Structures, 2004, 82(17–19), 1349–1358.

[6] Abdullah S.H., The buckling of an orthotropic composite truncated conical shell with continuously varying thickness subject to a time dependent external pressure, Composites: Part B, 2003, 34, 227–233.

[7] Bhimaraddi A., Carr J, Moss P.J., A shear deformable finite element for the analysis of general shells of revolution, Composite Structures, 1989, 31(3), 229–308.

[8] Singh B.N., Jibumon B Babu., Thermal buckling of laminated composite conical shell panel with and without piezoelectric layer with random material properties, International Journal of Crashworthiness, 2009, 14(1), 73–81.

[9] Singh B.N, Jibumon B Babu., Thermal buckling of laminated conical shells embedded with and without a piezoelectric layer, Journal of Reinforced Plastics and Composites, 2008,28(7): 791–812.

[10] Xu C.S., Xia Z.Q., Chia C.Y., Non-linear theory and vibration analysis of laminated truncated, thick conical shells. International Journal of Nonlinear Mechanisms 1996, 31(2), 139–154.

[11] Chen C., Dai L., Nonlinear vibration and stability of a rotary truncated conical shell with intercoupling of high and low order modals, Nonlinear Science and Numerical Simulation, 2009, 254–269.

[12] Ganesan N, Kadoli R, Buckling and dynamic analysis of piezothermoelastic composite cylindrical shell. Composite Structures, 2002, 59(1), 45–60.

[13] Omer Civalek. Numerical analysis of free vibrations of laminated composite conical and cylindrical shells: Discrete singular convolution (DSC) approach. Journal of Computer & Applied Mathematics 2007, 251–271.

[14] Franco Correia V.M, Mota Soares C.M., Mota Soares C.A., Higher order models on the eigen frequency analysis and optimal design of laminated composite structures, Composite Structures, 1997, 39(3-4), 237–253.

[15] Hu X.X., Sakiyama T., Matsuda H., Morita C., Vibration of twisted laminated conical shells, International Journal of Mechanical Science, 2002, 44, 1521–1541.

[16] Zhao X., Liew K.M., Free vibration analysis of functionally graded conical shell panels by a meshless method, Composite Structures, 2011, 93, 649–664.

[17] Jones R.M., Mechanics of composite materials, MCGraw-Hill, New York, 1975.

[18] Reddy J.N., Liu C.F., A higher order shear deformation theory of laminated elastic shells, International Journal of Engineering Sciences, 1985, 23(3), 319–330.

[19] Shankara C.A., Iyengar N.G.R., A $C^0$ element for the free vibration analysis of laminated composite plate. Journal of Sound and Vibration 1996, 191(5), 721–738.

[20] Padmanav Dash, Singh B.N., the Nonlinear free vibration of the piezoelectric laminated composite plate, Finite Element in Analysis and Design, 2009, 45, 686–694.

[21] Vivek Tripathi, Singh B.N., Shukla KK. Free vibration of laminated composite conical shells with random material properties, Composite Structures, 2007, 81(1), 96–104.

[22] Sofiyev AH, Kuruoglu N, Halilov HM. The vibration and stability of non-homogeneous orthotropic conical shells with clamped edges subjected to uniform external pressures. Applied Mathematical Modeling 2010, 34(7), 1807–1822.

[23] Chih-Ping Wu, Yi-Feng Pu, Yi-Hwa Tsai. Asymptotic solutions of axisymmetric laminated conical shells, Thin-Walled Structures 2005, 43(10), 1589–1614.

[24] Korjakin A., Rikards R., Chate A., Altenbach H., Analysis of free damped vibrations of laminated composite conical shells, Composite Structures, 1998, 41(1), 39–47.

[25] Chang C.H., Vibration of conical shells. Shock and Vibration Digest 1981, 13, 9–17.

[26] Bardell NS, Dunsdon JM, Langley RS. Free vibration of thin, isotropic, open, conical panels. Journal of Sound and Vibration 1998, 217, 297–320.

[27] Lim C.W., Liew K.M., Kitipornchai K., Vibration of cantilevered laminated composite shallow conical shells, International Journal of Solids and Structures, 1998, 35, 1695–1707.

[28] Singh B.N., Yadav D., Iyengar N.G.R., Natural frequencies of composite plates with random material properties using higher-order shear deformation theory, International Journal of Mechanical Science, 2001, 43, 2193–2214.

[29] Lim C.W., Liew K.M., Vibration behavior of shallow conical shells by global Ritz formulation. Engineering Structures, 1995, 17(1), 63–70.

[30] Achchhe Lal, Paras Choski, B.N. Singh, Stochastic nonlinear free vibration analysis of piezolaminated composite conical shell panel subjected to thermoelectromechanical loading with random material properties 2012,79, 1–17.

[31] Achchhe Lal, Nikhil M. Kulkarni, B.N. Singh, Stochastic Thermal post buckling response of elastically supported laminated piezoelectric composite plate using micromechanical approach, Curved and Layer. Struct., 2015, 2 (1), 331–350.

[32] Virendra Kumar Chaudhari, Niranjan L. Shegokar, and Achchhe Lal, Nonlinear free vibration analysis of elastically supported carbon nanotube-reinforced composbeam with the thermal environment in non-deterministic framework, Curved and Layer. Struct., 2017, 4:85–103.

[33] Zhao X., Li Q., Liew K.M., Ng T.Y., The element-free kpkp-Ritz method for free vibration analysis of conical shell panels, Journal of Sound and Vibration, 2006, 295(3–5), 906–922.

[34] Najmeh Jooybar, Parviz Malekzadeh, Alireza Fiouz, Mohammad Vaghefi, Thermal effect on free vibration of functionally graded truncated conical shell panels, Thin-Walled Structures, 2016, 103, 45–61.

[35] Rajsekaran S, Murray. Incremental finite element matrices. ASCE Journal of Structural Division 99, 1973, 2423–2438.

[36] Cook R.D., Malkus D.S., Plesha M.E., Concept and application of Finite Element Analysis. $3^{rd}$ edition. John Wiley and Sons; 1989.

# Appendix

$$H_{mn} = \begin{bmatrix} 1 & 0 & 0 & z & 0 & 0 & z^3 & 0 & 0 & 0 & 0 & 0 & 0 \\ 0 & 1 & 0 & 0 & z & 0 & 0 & z^3 & 0 & 0 & 0 & 0 & 0 \\ 0 & 0 & 1 & 0 & 0 & z & 0 & 0 & z^3 & 0 & 0 & 0 & 0 \\ 0 & 0 & 0 & 0 & 0 & 0 & 0 & 0 & 0 & 1 & 0 & z^2 & 0 \\ 0 & 0 & 0 & 0 & 0 & 0 & 0 & 0 & 0 & 0 & 1 & 0 & z^2 \end{bmatrix}, \tag{A.1}$$

$$H_{mn\phi} == \begin{bmatrix} 1 & 0 & z & 0 & z^2 & 0 & 0 & 0 \\ 0 & 1 & 0 & z & 0 & z^2 & 0 & 0 \\ 0 & 0 & 0 & 0 & 0 & 0 & 1 & z \end{bmatrix}. \tag{A.2}$$

$$S_{kl} = \begin{bmatrix} 1 & 0 & 0 & 0 & f_2(z) & 0 & f_1(z) \\ 0 & 1 & 0 & f_2(z) & 0 & f_1(z) & 0 \\ 0 & 0 & 1 & 0 & 0 & 0 & 0 \end{bmatrix}, \tag{A.3}$$

$$D_{mn} = \begin{bmatrix} A1_{ij} & B_{ij} & E_{ij} & 0 & 0 \\ B_{ij} & D1_{ij} & F1_{ij} & 0 & 0 \\ E_{ij} & F1_{ij} & H_{ij} & 0 & 0 \\ 0 & 0 & 0 & A2_{ij} & D2_{ij} \\ 0 & 0 & 0 & D2_{ij} & F2_{ij} \end{bmatrix} \tag{A.4}$$

Where

$$(A1_{ij}, B_{ij}, D1_{ij}, E_{ij}, F1_{ij}, H_{ij}) = \int_{-h/2}^{h/2} \overline{Q}_{ij} \left(1, z, z^2, z^3, z^4, z^6\right) dz \quad (i, j = 1, 2, 6)$$

$$(A2_{ij}, D2_{ij}, F2_{ij}) = \int_{-h/2}^{h/2} \overline{Q}_{ij} \left(1, z^2, z^4\right) dz \quad (i, j = 4, 5)$$

$$\left[D_{ijkl}^{NL}\right] = \begin{bmatrix} [0] & [0] & [0] & [M_1] & [N_1] \\ [0] & [0] & [0] & [N_1] & [P_1] \\ [0] & [0] & [0] & [Q_1] & [R_1] \\ [M_2] & [N_2] & [P_2] & [0] & [0] \\ [P_2] & [Q_2] & [R_2] & [0] & [0] \end{bmatrix}, \tag{A.5}$$

with $\left(M_{1_{ij}}, \quad N_{1_{ij}}, \quad P_{1_{ij}}, \quad Q_{1_{ij}}, \quad R_{1_{ij}}\right) = \sum_{k=1}^{NL} \int_{-h/2}^{h/2} e_{ij}^{(k)} \left(1, \quad z, \quad z^2, \quad z^3, \quad z^4\right) dz,$

where $i = 3, j = 1, 2, 6,$

$\left(M_{2_{ij}}, \quad N_{2_{ij}}, \quad P_{2_{ij}}, \quad Q_{2_{ij}}, \quad R_{2_{ij}}\right) = \sum_{k=1}^{NL} \int_{-h/2}^{h/2} e_{ij}^{(k)} \left(1, \quad z, \quad z^2, \quad z^3, \quad z^4\right) dz,$

where $i = 1, 2, j = 4, 5$

$$[D_3] = \begin{bmatrix} [A_1] & 0 \\ [B] & 0 \\ [E] & 0 \\ 0 & [A_2] \\ 0 & [C_2] \end{bmatrix}, \quad [D_4] = [D_3]^T \quad \text{and} \quad [D_5] = \begin{bmatrix} [A_1] & 0 \\ 0 & [A_2] \end{bmatrix} \tag{A.6}$$

$$\left\{B_{ij}^{\alpha}\right\} = \begin{Bmatrix} \varepsilon_1^0 \\ \varepsilon_2^0 \\ \varepsilon_6^0 \\ k_1^0 \\ k_2^0 \\ k_6^0 \\ k_1^2 \\ k_2^2 \\ k_6^2 \\ \varepsilon_4^0 \\ \varepsilon_5^0 \\ k_4^2 \\ k_5^2 \end{Bmatrix} = \begin{bmatrix} N_{i,s} & 0 & 0 & 0 & 0 & 0 & 0 \\ 0 & N_{i,\theta} & 1/R_\theta & 0 & 0 & 0 & 0 \\ N_{i,\theta} & N_{i,s} & 0 & 0 & 0 & 0 & 0 \\ 0 & 0 & 0 & 0 & 0 & 0 & C_1 N_{i,s} \\ 0 & 0 & 0 & 0 & 0 & C_1 N_{i,\theta} & 0 \\ 0 & 0 & 0 & 0 & 0 & C_1 N_{i,s} & C_1 N_{i,\theta} \\ 0 & 0 & 0 & 0 & -C_4 N_{i,s} & 0 & -C_2 N_{i,s} \\ 0 & 0 & 0 & -(C_4/R_\theta) N_{i,\theta} & 0 & -C_2 N_{i,\theta} & 0 \\ 0 & 0 & 0 & -C_4 N_{i,s} & -C_4 N_{i,\theta} & -C_2 N_{i,s} & -C_2 N_{i,\theta} \\ 0 & 0 & C_1 N_{i,\theta} & 0 & 0 & C_1 & 0 \\ 0 & 0 & C_1 N_{i,s} & 0 & 0 & 0 & C_1 \\ 0 & 0 & 0 & -3C_4/R_\theta & 0 & -3C_2 & 0 \\ 0 & 0 & 0 & 0 & -3C_4 & 0 & -3C_2 \end{bmatrix} \begin{Bmatrix} s \\ \theta \\ z \\ \theta_\theta \\ \theta_s \\ \beta_\theta \\ \beta_s \end{Bmatrix}, \tag{A.7}$$

$$\overline{N}_0^T = \begin{bmatrix} N_s^T & M_s^T \\ N_\theta^T & M_\theta^T \\ N_{s\theta}^T & M_{s\theta}^T \end{bmatrix} = \sum_{k=1}^{NL} \int_{-h/2}^{h/2} \begin{bmatrix} A_s \\ A_\theta \\ A_{s\theta} \end{bmatrix} (1, z)\, \Delta T dz \tag{A.8}$$

$$\overline{N}_0^V = \begin{bmatrix} N_s^V & M_s^V \\ N_\theta^V & M_\theta^V \\ N_{s\theta}^V & M_{s\theta}^V \end{bmatrix} = \sum_{k=1}^{NL} \int_{-h/2}^{h/2} \begin{bmatrix} B_s \\ B_\theta \\ B_{s\theta} \end{bmatrix} (1, z)\, \frac{Vk}{tk} dz \tag{A.9}$$

where

$$\begin{bmatrix} A_s \\ A_\theta \\ A_{s\theta} \end{bmatrix} = - \begin{bmatrix} \overline{Q_{11}} & \overline{Q}_{12} & \overline{Q}_{16} \\ \overline{Q}_{12} & \overline{Q}_{22} & \overline{Q}_{26} \\ \overline{Q}_{16} & \overline{Q}_{26} & \overline{Q}_{66} \end{bmatrix} \begin{bmatrix} c^2 & s^2 \\ s^2 & c^2 \\ 2cs & -2cs \end{bmatrix} \begin{bmatrix} \alpha_{11} \\ \alpha_{22} \end{bmatrix}$$

$$\begin{bmatrix} B_s \\ B_\theta \\ B_{s\theta} \end{bmatrix} = - \begin{bmatrix} \overline{Q_{11}} & \overline{Q}_{12} & \overline{Q}_{16} \\ \overline{Q}_{12} & \overline{Q}_{22} & \overline{Q}_{26} \\ \overline{Q}_{16} & \overline{Q}_{26} & \overline{Q}_{66} \end{bmatrix} \begin{bmatrix} c^2 & s^2 \\ s^2 & c^2 \\ 2cs & -2cs \end{bmatrix} \begin{bmatrix} d_{31} \\ d_{32} \end{bmatrix}$$

$$D_{1P} = \begin{bmatrix} [0] & [0] & [0] & [M_1] & [N_1] \\ [0] & [0] & [0] & [N_1] & [P_1] \\ [0] & [0] & [0] & [Q_1] & [R_1] \\ [M_2] & [N_2] & [P_2] & [0] & [0] \\ [P_2] & [Q_2] & [R_2] & [0] & [0] \end{bmatrix}, \tag{A.10}$$

with $\left(M_{1_{ij}},\quad N_{1_{ij}},\quad P_{1_{ij}},\quad Q_{1_{ij}},\quad R_{1_{ij}}\right) = \sum_{k=1}^{NL} \int_{z_{k-1}}^{z_k} e_{ij}^{(k)} \left(1,\quad z,\quad z^2,\quad z^3,\quad z^4\right) dz$, where $i = 3, j = 1, 2, 6$

$\left(M_{2_{ij}},\quad N_{2_{ij}},\quad P_{2_{ij}},\quad Q_{2_{ij}},\quad R_{2_{ij}}\right) = \sum_{k=1}^{NL} \int_{z_{k-1}}^{z_k} e_{ij}^{(k)} \left(1,\quad z,\quad z^2,\quad z^3,\quad z^4\right) dz$, where $i = 1, 2, j = 4, 5$

$$D_{2P} = \begin{bmatrix} [S_1] & [T_1] & [U_1] & [0] & [0] \\ [T_1] & [U_1] & [V] & [0] & [0] \\ [U_1] & [V] & [W] & [0] & [0] \\ [0] & [0] & [0] & [S_2] & [T_2] \\ [0] & [0] & [0] & [T_2] & [U_2] \end{bmatrix}, \tag{A.11}$$

with

$\left(S_{1_{ij}},\quad T_{1_{ij}},\quad U_{1_{ij}},\quad V_{ij},\quad W_{ij}\right) = \sum_{k=1}^{NL} \int_{z_{k-1}}^{z_k} k_{ij}^{(k)} \left(1,\quad z,\quad z^2,\quad z^3,\quad z^4\right) dz$, where $i, j = 1, 2$

$$\left(S_{2_{ij}},\quad T_{2_{ij}},\quad U_{2_{ij}}\right)=\sum_{k=1}^{NL}\int_{z_{k-1}}^{z_k}k_{ij}^{(k)}\left(1,\quad z,\quad z^2\right)dz,\ \text{where } i,j=3$$

$$D_6=\begin{bmatrix}0&0&0&M_1&N_1\\M_2&N_2&P_2&0&0\end{bmatrix},\ D_7=\begin{bmatrix}0&M_2\\0&N_2\\0&P_2\\M_1&0\\N_1&0\end{bmatrix}, \tag{A.12}$$

$$\left[M_{jk}\right]=\sum_{k=1}^{NL}\int_{z_{k-1}}^{z_k}\rho^{(k)}\left[\overline{N}\right]^T\left[\overline{N}\right]dz,$$

$$\left[\bar{N}\right]=\begin{bmatrix}1&0&0&0&f_2(z)&0&f_1(z)\\0&(1+z/R_\theta)^2&0&f_2(z)(1+z/R_\theta)&0&f_1(z)/R_\theta(1+z/R_\theta)&0\\0&0&1&0&0&0&0\\0&f_2(z)(1+z/R_\theta)&0&f_2^2(z)&0&f_1(z)f_2(z)/R_\theta&0\\f_2(z)&0&0&0&f_2^2(z)&0&f_1(z)f_2(z)\\0&f_1(z)/R_\theta(1+z/R_\theta)&0&f_1(z)f_2(z)/R_\theta&0&f_1^2(z)/R_\theta^2&0\\f_2(z)&0&0&0&f_1(z)f_2(z)&0&f_1^2(z)\end{bmatrix}. \tag{A.13}$$